Acta Cryst. (1958). **11**, 139

Imperfections in Hexagonal Cobalt*

By C. R. Houska and B. L. Averbach

Department of Metallurgy, Massachusetts Institute of Technology, Cambridge, Massachusetts, U.S.A.

(*Received* 26 *June* 1957)

The influence of local strain, fine particle size, and stacking faults on the diffraction pattern of hexagonal cobalt have been considered. Quantitative X-ray measurements showed that hexagonal cobalt produced by transformation was relatively free of local strain and particle-size effects, but both growth and deformation faults were observed. It was also found that this hexagonal structure was composed of two types of material: one region contained random deformation faults; the other region contained both random deformation and growth faults. The relative fraction of the two materials was measured but the distribution of these two types of materials could not be determined. Cobalt specimens which were highly deformed and subsequently annealed without transformation contained a homogeneous distribution of random growth and deformation faults. It was also shown that extended dislocations would produce X-ray diffraction effects which were not observed.

1. Introduction

Hexagonal cobalt is formed from f.c.c. cobalt by a transformation which is martensitic on cooling below a temperature of about 390° C. The work of Edwards & Lipson (1942) and Wilson (1942) clearly demonstrated the presence of stacking faults in hexagonal cobalt. It was later suggested (Christian, 1954; Anantharaman & Christian, 1956) that two types of stacking faults can be formed, a growth fault and a deformation fault. The latter defect was not considered in the earlier work, and Christian carried out the diffraction calculations for this effect. Gevers (1954) has treated the more general case in which both types of stacking faults occur.

A number of open questions remain on the faulted cobalt structure, and this study attempts to answer some of them. The general diffraction problem for hexagonal materials wherein effects arising from localized strains, fine particle size, and stacking faults of both kinds, is investigated by extending Warren's treatment of cold work (1955). The question of the randomness of the stacking faults is also considered The diffraction effects arising from the presence of extended dislocations is treated by considering the stacking sequence of cells arranged in columns. Within each column some cells do not follow the normal sequence because of the presence of a stacking fault, whereas a column which does not intercept the extended dislocation has a normal sequence and this allows the calculation of the effects arising from an extended dislocation.

Quantitative line-shape determinations were made on several cobalt specimens, and the application of the diffraction analysis permitted quite definite conclusions with respect to the types, distribution, and fraction of defects present under specified conditions in hexagonal cobalt.

* This work was carried out under the sponsorship of the U.S. Atomic Energy Commission.

2. Diffraction theory

For a perfect hexagonal material the relative atomic positions can be described by the vector

$$R_m = (n_1+X_{n_3})a_1+(n_2+Y_{n_3})a_2+n_3a_3\,, \qquad (1)$$

where a_1, a_2, and a_3 (which is equal to $\frac{1}{2}c$) are hexagonal axes; n_1, n_2 and n_3 are integers; X_{n_3} and Y_{n_3} are definite fractions which describe the stacking sequence of close-packed planes along a_3. In the more general case, in which imperfections are present, the stacking sequence is interrupted by mistakes, and atoms are further displaced by internal strains. Consequently, the fractions X_{n_3} and Y_{n_3} must be generalized to include the possibility of finding layer cells in the wrong sequence and also to include the effect of local distortions. In addition, a strain component, Z_n, parallel to a_3 must be included, i.e.

$$R_m-R_{m'} = (X_n+n_1)a_1+(Y_n+n_2)a_2+(Z_n+n_3)a_3\,, \qquad (2)$$

where n is an abbreviation for $(n_1n_2n_3)$ since the displacements must have a three-dimensional dependence. Substituting this into the intensity expression

$$I = I_e f^2 \sum_m \sum_{m'} \exp 2\pi i H\,.\,(R_m-R_{m'})\,, \qquad (3)$$

where, $H = h_1b_1+h_2b_2+h_3b_3$, and b_1, b_2, b_3 are reciprocal vectors to a_1, a_2, a_3 respectively, we obtain

$$I = I_e f^2 \sum_{n_1}\sum_{n_2}\sum_{n_3} \exp 2\pi i H\,.\,\delta_n \times \exp 2\pi i\,(n_1h_1+n_2h_2+n_3h_3) \qquad (4)$$

with $\delta_n = X_na_1+Y_na_2+Z_na_3$, and the summations are taken over all atom pairs. For each lattice vector having components $(n_1n_2n_3)$, there is an associated

sum of exponential terms formed by considering the individual displacements of all $(m-m')$ atom pairs. The summation can be written in terms of an average exponential and the total number of such terms, N_n, i.e.

$$I = I_e f^2 \sum_{n_1}\sum_{n_2}\sum_{n_3} N_n \langle \exp 2\pi i H.\delta_n \rangle \times \exp 2\pi i (n_1h_1+n_2h_2+n_3h_3) . \quad (5)$$

It will be assumed that the reflections are sharp enough such that $h_1 = h$, $h_2 = k$, and $h_3 = l$ in the averaging.

The total diffracted power from a reflection is given by

$$P = \frac{MjR^2\lambda^3}{4V_a}\iiint \frac{I}{\sin\theta}\, dh_1 dh_2 dh_3 , \quad (6)$$

where I is the intensity per crystal, M is the number of diffracting crystals, j is the multiplicity, R is the specimen-to-receiver distance, λ is the wavelength, and V_a is the volume of the unit cell. The required integrations cannot be carried out conveniently with the present system of axes. It has been shown by Warren (1955) that a general system of axes can be transformed by a suitable matrix transformation to give a new set with two of the three axes parallel to the reflecting sphere. Using this set, it is possible to obtain an expression for a powder pattern. Let b_1', b_2', b_3' represent the rotated set; a_1', a_2', a_3' the corresponding crystalline set. Making these substitutions gives the result

$$P = K\iiint \sum_{n_1'}\sum_{n_2'}\sum_{n_3'} A_{n'}^P A_{n'} \times \exp 2\pi i (n_1'h_1'+n_2'h_2'+n_3'h_3') dh_1'' dh_2'' dh_3'' \quad (7)$$

where

$K = I_e f^2 MNjR^2\lambda^3/4V_a \sin\theta$,*
N = total number of atoms per crystal,
$A_{n'}^P = N_{n'}/N$,
$A_{n'} = \langle \exp 2\pi i H.\delta_{n'} \rangle$

and h_1'', h_2'' refer to distances from the points of reflection in reciprocal space in units of b_1', b_2'. Integrating over all contributions to the Bragg reflection with respect to h_1'' and h_2'' from $-w$ to $+w$ gives

$$P = K\int \sum_{n_1'}\sum_{n_2'}\sum_{n_3'} A_{n'}^P A_{n'} \frac{\sin \pi n_1' w}{\pi n_1'} \frac{\sin \pi n_2' w}{\pi n_2'} \times \exp 2\pi i n_3' h_3' dh_3' . \quad (8)$$

The two sums of the form

$$\sum_{n_1'} \frac{\sin \pi n_1' w}{\pi n_1'}$$

are significant mainly at $n_1' = n_2' = 0$. Therefore,

$$P = K\int \sum_{n_3'} A_{n_3'}^P A_{n_3'} \exp 2\pi i n_3' h_3' dh_3' . \quad (9)$$

* $\sin\theta$ can be taken as a constant for a given reflection.

The equation

$$dh_3' = |a_3'| \frac{\cos\theta}{\lambda} d(2\theta) \quad (10)$$

provides the change in variable for the total power density in terms of 2θ. Dividing by $2\pi R \sin 2\theta$ gives the final form in terms of the diffracted power per unit arc length and angular increment, i.e.

$$P'(2\theta) = K' \sum_{n_3'} A_{n_3'}^P A_{n_3'} \exp 2\pi i n_3' h_3' \quad (11)$$

with

$$K' = MNjR\lambda^2 f^2 a_3' I_e / 16\pi V_a \sin^2\theta .$$

The term $A_{n_3'}$ contains both strain and stacking coordinates. In taking this average, it is simpler to think of the product $(H.\delta_{n_3'})$ in terms of the untransformed axes but with a vector separation $n_3'a_3'$ between cells. The averages are taken with respect to the cells in each column taken separately and not from one column to another, since $n_1' = n_2' = 0$.

3. Interpretation of Fourier coefficients

The Fourier coefficients in (11) appear as a product of a particle-size coefficient and a coefficient involving both the stacking and distortion coordinates. The latter is not in the most convenient form and will be considered in greater detail.

For a perfect hexagonal sequence ($A\,B\,A\,B\,A$ type), the stacking coordinates take values:

(X_k, Y_k, Z_k) = $(0, 0, 0)$, if k corresponds to an even layer
= $(\pm\frac{2}{3}, \pm\frac{1}{3}, 0)$, if k corresponds to an odd layer.

In the latter case, the sign depends upon whether the reference layer is an A or B. For an $[hk0]$ direction all cells are of a $(0, 0, 0)$ type and none is in $(\pm\frac{2}{3}, \pm\frac{1}{3}, 0)$ positions, since no extended dislocation patches are present in the perfect material.

We now consider the case in which extended dislocations are scattered throughout the material. In this case, the strain terms x_k, y_k, and z_k should also be included. In addition, it is possible to find all three types of stacking displacements for any $\langle hkl \rangle$ direction including $\langle hk0 \rangle$, i.e.

$$(X_k, Y_k, Z_k) = (x_k, y_k, z_k) \quad (A)$$
$$= (\tfrac{2}{3}+x_k, \tfrac{1}{3}+y_k, z_k) \quad (B)$$
$$= (-\tfrac{2}{3}+x_k, -\tfrac{1}{3}+y_k, z_k) . \quad (C)$$

The calculations are greatly simplified if the strain coordinates are assumed to be independent of the stacking coordinates. This is a reasonable assumption provided the strain centers are not associated with the stacking faults, and a certain fraction of the strain centers are probably of this type. If the faulted cells result from extended dislocations in the usual sense,

then each partial dislocation associated with an extended dislocation is a strain center. Consequently, it does not seem justified to assume the strain centers to be entirely independent of the stacking coordinates. However, it should be recognized that each of the partial dislocation cores represents a discontinuity between a faulted region and an unfaulted region, and that each region is strained by the partial. On this basis, the strain term for both a faulted and its adjacent unfaulted region should not be significantly different in magnitude. Consequently, the same strain term will be used irrespective of the stacking coordinate.

Stacking and strain probabilities are defined in the following manner: $P^0_{n_3'}$, $P^+_{n_3'}$ and $P^-_{n_3'}$ are the probabilities for finding the relative translations (0, 0, 0), $(\frac{2}{3}, \frac{1}{3}, 0)$, and $(-\frac{2}{3}, -\frac{1}{3}, 0)$ respectively at a separation of $n_3'a_3'$. The quantity $P_{n_3'}dxdydz$ represents the probability of finding a strain between x, y, z and $x+dx$, $y+dy$, $z+dz$ at a spacing $n_3'a_3'$. Taking the average with respect to these definitions:

$$\langle \exp 2\pi i H.\delta_{n_3'}\rangle$$
$$= \{P^0_{n_3'}+P^+_{n_3'} \exp 2\pi i(\tfrac{2}{3}h+\tfrac{1}{3}k)+P^-_{n_3'} \exp -2\pi i(\tfrac{2}{3}h+\tfrac{1}{3}k)\}$$
$$\times \iiint P_{n_3'} \exp 2\pi i(x_{n_3'}h+y_{n_3'}k+z_{n_3'}l)\,dx\,dy\,dz \quad (12)$$
$$= \{P^0_{n_3'}+P^+_{n_3'} \exp 2\pi i(\tfrac{2}{3}h+\tfrac{1}{3}k)+P^-_{n_3'} \exp -2\pi i(\tfrac{2}{3}h+\tfrac{1}{3}k)\}$$
$$\langle \exp 2\pi i(x_{n_3'}h+y_{n_3'}k+z_{n_3'}l)\rangle . \quad (13)$$

Let $A^{SF}_{n_3'} = P^0_{n_3'}+P^+_{n_3'}$
$$\times \exp 2\pi i(\tfrac{2}{3}h+\tfrac{1}{3}k)+P^-_{n_3'} \exp -2\pi i(\tfrac{2}{3}h+\tfrac{1}{3}k)$$
and
$$A^D_{n_3'} = \langle \exp 2\pi i(x_{n_3'}h+y_{n_3'}k+z_{n_3'}l)\rangle .$$

For reflections of the type $h-k = 3t$ (t = integer),

$$A^{SF}_{n_3'} = 1{\cdot}00 \text{ since } P^0_{n_3'}+P^+_{n_3'}+P^-_{n_3'} = 1{\cdot}00.$$

For $h-k = 3t\pm1$, we obtain

$$A^{SF}_{n_3'} = (\tfrac{3}{2}P^0_{n_3'}-\tfrac{1}{2})+i\tfrac{1}{2}\sqrt{3}(P^+_{n_3'}-P^-_{n_3'}) . \quad (14)$$

Reflections of this type are affected by the stacking sequence for all values of l, including $l = 0$. Thus, only certain lines are broadened by the presence of extended dislocations in hexagonal materials, and a discontinuous line broadening for reflections of the type $(hk0)$ where $h-k = 3t\pm1$ has not been predicted previously. It results from the mistakes within individual close-packed layers. The effect is, of course, proportional to the average number of extended dislocation patches within a layer. If the patches are large and widely spaced, the broadening is small.

Substituting the results of this section into equation (11) gives

$$P'_{(2\theta)} = K' \sum_{n_3'} A^P_{n_3'} A^{SF}_{n_3'} A^D_{n_3'} \exp 2\pi i n_3' h_3' . \quad (15)$$

This represents a Fourier series involving the product of three coefficients, each characteristic of one defect, i.e. particle size, faulted cells, and strains. A line broadening will be observed if any one of these coefficients decreases with increasing n_3'. It is possible in principle to separate these coefficients by making use of an extrapolation method (Warren & Averbach, 1952). If one considers reflections of the type $h-k=3t$, then $A^{SF}_{n_3'} = 1{\cdot}00$ and the above mentioned method can be used directly. It does not seem practical to employ such methods for the separation of $A^{SF}_{n_3'}$. A A more practical procedure is to assume a model for the particle-shape and strain distribution on the basis of the measurements obtained from reflections which are unaffected by stacking faults, and thereby obtain information concerning the stacking sequence. The final procedure must be adapted to the specific problem.

4. The powder pattern for transformed and annealed cobalt

Diffraction line shapes from 99·99% cobalt specimens were measured quantitatively. Powder briquettes were prepared by grinding solid cobalt with an alundum wheel; the cobalt was separated with a magnet. Briquettes were pressed and the specimen was annealed at 300° C. for 7 days and at 390° C. for 2 days. After this treatment the structure was entirely hexagonal. Detailed diffraction-line shapes were observed with a Geiger-counter spectrometer, using filtered Fe $K\alpha$ radiation. The sample was then heated quickly into the f.c.c. region (600° C.) and ice-quenched. In both cases it was found that lines of the type $(00l)$ and $(hk0)$ were sharp, with the $K\alpha_1$, $K\alpha_2$ doublet resolved at high Bragg angles. Since both strain and particle-size broadening increase with (2θ) (as $1/\cos\theta$ and $\tan\theta$ respectively), it would be expected that if either were present the high-angle lines should be broadened relative to the low-angle lines. This was not the case. Consequently, both strain and particle-size broadening could be neglected for these specimens. That is, the particle size is greater than about 1000 Å and the local strains are less than 1×10^{-3}. Therefore, $A^D_{n_3'} = A^{PS}_{n_3'} = 1{\cdot}00$. In addition, reflections of the type $h-k = 3t\pm1$ and $l = 0$ were not broadened relative to $h-k = 3t$ and $l = 0$. In the preceding section it was shown that two types of broadening should exist if stacking faults exist as extended dislocations. Neither broadening was observed. Thus, extended dislocations of the usual form are not present, or are present in very small numbers. If the extended dislocations are composed of partial dislocations located at the boundaries, then the volume strains are greatly reduced and the faults can be considered as entire misplaced planes.

Under these conditions, further simplifications can be made. It is unnecessary to use the rotated axes in making the integrations for a powder pattern. The

integrations can be made along b_1 and b_2 from $-w$ to $+w$ so as to include all the Bragg intensity in these directions at a given value of h_3b_3. This approximate integration is adequate except for reflections of the type ($hk0$). The powder pattern for all reflections except ($hk0$) can then be written as

$$P'_{(2\theta)} = K' \sum_{n_3} A_{n_3}^{SF} \exp 2\pi i n_3 h_3 \qquad (16)$$

where $h_3 = (2|a_3|/\lambda)(\sin^2\theta - \sin^2\theta_0)^{\frac{1}{2}}$, and θ_0 is the Bragg angle for ($hk0$). In all cases, it was possible to take K' as a constant. This enabled the ordinates of the pattern to be used directly after subtracting background. The Fourier coefficients of the (101), (102), and (103) are shown in Fig. 1 for the annealed

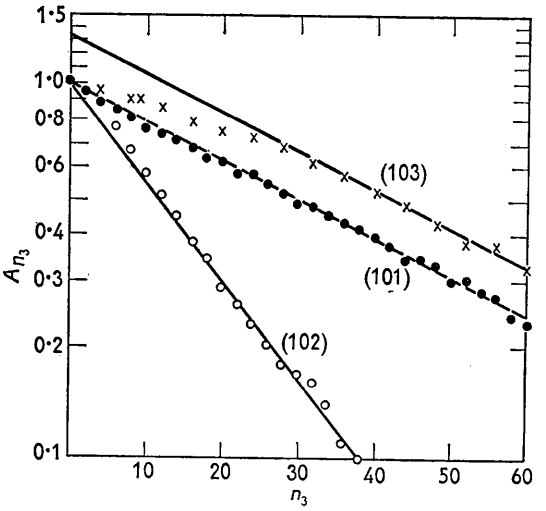

Fig. 1. Fourier coefficients. Sample ground at room temperature and annealed at 300° C. for 7 days and at 390° C. for 2 days.

specimen corrected for instrumental broadening by using the Stokes method (1948) and Lipson–Beever strips. In each case, the peak maximum was taken as the origin. The true origin is at $h_3 = 0$, consequently the origin must be shifted to this value for the (101) and (103) reflections by multiplying each coefficient by $(-1)^{n_3}$. No correction is necessary for the (102). One period along b_3 includes two reflections, either (101) and (102) or (102) and (103). Consequently the true periodicity along (hk) = (10) is

$$f_{(h_3)}^{10} = K_1 f_{(h_3)}^{(101) \text{ or } (103)} + K_2 f_{(h_3)}^{(102)}.$$

K_1 and K_2 can be evaluated from the initial conditions $P_0 = 1{\cdot}00$, $P_1^+ = P_1^- = 0{\cdot}50$, and give the values $K_1 = \frac{3}{4}$ and $K_2 = \frac{1}{4}$ if $A_0^{10} = A_1^{10} = 1{\cdot}00$.

Thus,

$$A_{n_3}^{SF}(10) = \tfrac{3}{4}(-1)^{n_3} A_{n_3}^{(101) \text{ or } (103)} + \tfrac{1}{4} A_{n_3}^{(102)}. \qquad (17)$$

Taking $P_{n_3}^+ = P_{n_3}^-$, equation (14) becomes

$$A_{n_3}^{SF} = \tfrac{1}{2}(3P_{n_3}^0 - 1) \qquad (18)$$

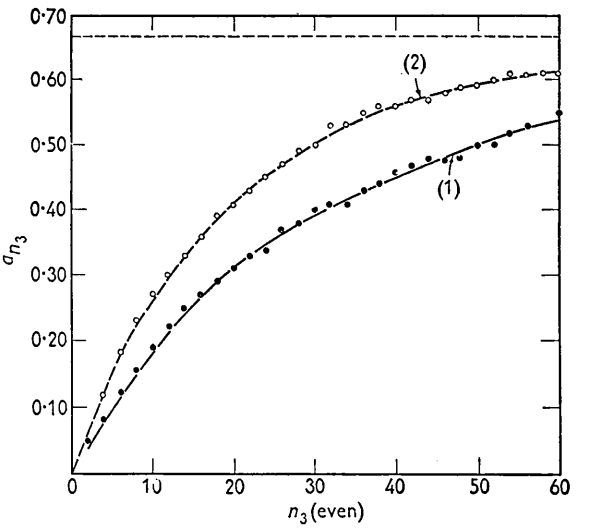

Fig. 2. Probability of finding a stacking fault in transformed and annealed cobalt powder.

Consecutive heat treatments for same sample: (1) Ground at room temperature and annealed at 300° C. for 7 days and at 390° C. for 2 days; transformation 100% h.c.p. (2) As for (1) followed by anneal at 600° C. for 15 min. and ice quench; transformation 81% h.c.p.

or

$$P_{n_3}^0 = \tfrac{1}{3}(2A_{n_3}^{SF} + 1) \qquad (18a)$$

for odd values of n_3. Since $P_{n_3}^0 = 0$ for the perfect material, equation (18a) represents the probability of finding a stacking fault at n_3 interlayer spacings. For even values of n_3,

$$\alpha_{n_3} = 1 - P_{n_3}^0 = \tfrac{2}{3}(1 - A_{n_3}^{SF}) \qquad (19)$$

represents the probability of finding a stacking fault at n_3 interlayer spacings. These results give the statistical picture of faulting without assuming the stacking sequence to be random. Typical plots of α_{n_3} are given in Fig. 2.

Tests can be made on the data which permit one to obtain information concerning the distribution of stacking faults. If the Fourier coefficients of the separate lines follow the relation $A_{n_3}(hkl) = A_1(hkl)^{|n_3|}$, then the distribution of faults can be considered as random (Méring, 1949; Houska & Warren, 1954). Fig. 1 indicates that this relation is satisfied for the (101) and (102) reflections. For the (103), the discrepancy at small values of n_3 results from the choice of background in making the Fourier analysis. Despite this, it is seen that at large n_3 values the slope is very close to that obtained from the (101), as is expected from theory. Since the plots are linear when background is well determined, the distribution of faults can be taken as random.

After having shown that the stacking faults occur at random, it is justifiable to make use of existing diffraction calculations which assume randomness.

The two defects which have been considered are represented schematically by the following sequences:

hex. hex.	hex. hex.
$\overbrace{A\,B\,A}\overbrace{B\,C\,B\,C\,B}$	$\overbrace{A\,B\,A}\overbrace{B\,C\,A\,C\,A\,C}$
$\underbrace{\quad}$ f.c.c.	$\underbrace{\quad}$ f.c.c.
1 growth fault	1 deformation fault

Let α represent the probability of finding a growth fault (i.e. three layers in the cubic sequence) and γ represent the probability of finding a deformation fault (i.e. the probability of finding partial slip between consecutive layers). These probabilities refer strictly to a random distribution of defects and consequently differ from the set α_{n_3}, which are meaningful for any distribution of defects. In the former case α and γ do not vary with increasing interplanar spacing whereas α_{n_3} increases. From (4) the coefficients for $h-k=3t\pm1$ can be written as:

$$\ln A_1^0 = -(\tfrac{1}{2}\alpha+\tfrac{3}{2}\gamma) \qquad (hkl = \text{odd}), \tag{20}$$

$$\ln A_1^e = -(\tfrac{3}{2}\alpha+\tfrac{3}{2}\gamma) \qquad (hkl = \text{even}). \tag{21}$$

From the slopes of the semi-logarithmic plots of

$$A_{n_3}^{(101)\text{ or }(103)} = (A_1^0)^{|n_3|} \text{ and } A_{n_3}^{(102)} = (A_1^e)^{|n_3|}$$

(see Fig. 1), $\alpha = 0{\cdot}036$ and $\gamma = 0{\cdot}004$.

For specimens of cobalt powder which were heated into the f.c.c. range and then transformed to hexagonal material by quenching, the preceding approach was not strictly applicable. A semi-log plot of the Fourier coefficients (Fig. 3) does not give a single straight line for the (102) reflection. Two straight line regions are apparent. Experimentally it was observed that the (102) line shape appeared as a superposition of a sharp line and a broad line. (This was also observed by Edwards & Lipson (1942).) This is consistent with the two linear regions of the coefficient plot. The Fourier coefficients can be explained by considering that the hexagonal structure contains two types of material:

1. One region contains only random deformation faults,
2. The other region contains random deformation and growth faults.

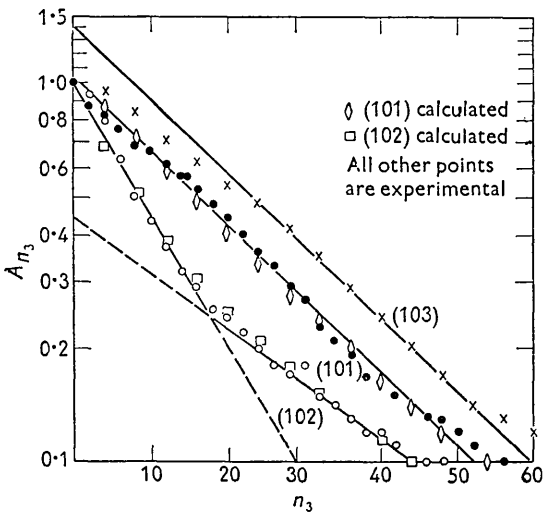

Fig. 3. Fourier coefficients. Same sample as in Fig. 1 but with additional anneal at 600° C. for 15 min. and ice quench.

If the two regions are large, the intensity can be expressed by the two series, i.e.

$$f_{(h3)}^{10} = \sum_{n_3} (k_1 A'_{n_3} + k_2 A''_{n_3}) \exp 2\pi n_3 h_3 ,$$

where

$$k_1+k_2 = 1,$$
$$A'_{n_3} = (A'_1)^{|n_3|} \quad \text{(for region of type (1))},$$
$$A''_{n_3} = (A''_1)^{|n_3|} \quad \text{(for region of type (2))}.$$

For l odd we have

$$\ln A'_1 = -\tfrac{3}{2}\gamma^{(1)},$$
$$\ln A''_1 = -\tfrac{1}{2}\alpha^{(2)}-\tfrac{3}{2}\gamma^{(2)},$$

and for l even we have

$$\ln A'_1 = -\tfrac{3}{2}\gamma^{(1)},$$
$$\ln A''_1 = -\tfrac{3}{2}\alpha^{(2)}-\tfrac{3}{2}\gamma^{(2)}.$$

The probabilities are defined as:

- $\gamma^{(1)}$ is the probability of finding a deformation fault in material (1),
- $\gamma^{(2)}$ is the probability of finding a deformation fault in material (2),
- $\alpha^{(2)}$ is the probability of finding a growth fault in material (2).

The following values were obtained by curve-fitting:

$$\gamma^{(1)} = 0{\cdot}023, \quad \alpha^{(2)} = 0{\cdot}080, \quad \gamma^{(2)} = 0{\cdot}014,$$
$$k_1 = 0{\cdot}45, \quad k_2 = 0{\cdot}55 .$$

Fig. 3 illustrates that the Fourier coefficients are well represented by the calculated points obtained by making use of the preceding values and assumptions.

5. Discussion

The generalized X-ray treatment of the effects on the line shape of hexagonal structures introduced by the presence of localized strains, particle-size and stacking faults has shown that these influences appear in the Fourier coefficients of a function which describes the line shape. These are difficult to separate in cases where all three effects are present, and the experimental work on cobalt was confined to cases wherein the particle-size and local-strain effects were negligible. A study of the stacking-fault coefficients, however, indicated that the separate probabilities for finding deformation faults and growth faults could be observed.

Two types of hexagonal cobalt structures were studied. In one case the specimen was partially transformed by cooling to room temperature and the remainder of the transformation to the hexagonal structure was carried out by deformation during the grinding of fine powders. The hexagonal cobalt was then annealed to relieve the local strains and to increase the particle size, and the resultant structure was analyzed for the presence of stacking faults. In the second type of experiment the hexagonal structure was reheated into the f.c.c. phase and quenched into ice water. The resultant structure was a mixture of hexagonal cobalt formed by transformation on cooling below the M_s temperature and retained f.c.c. structure.

It has shown that strain broadening and particle-size broadening could also be neglected in the case of the hexagonal structure formed on transformation. This indicates that the average particle size in any direction is probably greater than 1000 Å and the root mean square average strains are smaller than 1×10^{-3}. Consequently, there are relatively small local disturbances associated with the martensite transformation in this case. This is not unexpected since the transformation f.c.c. → hexagonal involves mainly a change in the stacking sequence and only very small adjustments in the lattice structure. It was also observed that reflections of the type $h-k = 3t \pm 1$ and $l \neq 0$ were broadened, whereas all other reflections were sharp. The combined absence of the discontinuous broadening of ($hk0$) reflections and the absence of strain broadening indicate that extended dislocations cannot be present in large quantities in these specimens unless the partial dislocations are contained in the boundaries of the sub-grains. The latter picture is identical to the case in which the faulted planes extend over the entire sub-grain.

A general distribution of stacking faults was obtained in which the stacking-fault probability was found at various interlayer spacings. This distribution is a statistical representation of the distribution of stacking faults in the hexagonal phase of a cobalt powder. As it stands, it does not give directly the type of distribution present in the hexagonal phase. To obtain this, tests must be made directly upon this curve or upon the Fourier coefficients which describe the shape of the individual reflections. In the case of a random distribution of faults the Fourier coefficients take the form $A_{n3} = A_1^{|n3|}$. This was found to be the case for the annealed hexagonal specimen. The probability of finding a growth fault was 0·036 while the probability of finding a deformation fault was 0·004

The distribution of faults for a hexagonal cobalt specimen formed by transformation on cooling is more complex. The simple exponential relationship between the Fourier coefficients of various orders was not found. A second term was required to fit the data and this can be interpreted as showing that the transformed cobalt consists of two regions; one region contains only deformation faults, the other region contains both deformation and growth faults. The faults were randomly distributed in each material. The transformed cobalt contained about 50% of each type of material. The probability of finding a deformation fault in the first material was 0·023. The probability of finding a deformation fault in the second material was 0·014, but the probability of finding a growth fault in the second material was 0·080. This indicates that growth faults are very prevalent, and these may be a consequence of the joining up of various sub-grains in the martensitic phase. The deformation faults are considerably less prevalent and these may be a consequence of the local deformation associated with the transformation. A later paper will deal more completely with the transformation characteristics.

The authors are grateful to the Atomic Energy Commission for their sponsorship of this research.

References

ANANTHARAMAN, T. R. & CHRISTIAN, J. W. (1956). *Acta Cryst.* **9**, 479.
CHRISTIAN, J. W. (1954). *Acta Cryst.* **7**, 415.
EDWARDS, O. S. & LIPSON, H. (1942). *Proc. Roy. Soc.* A, **180**, 268.
GEVERS, R. (1954). *Acta Cryst.* **7**, 337.
HOUSKA, C. R. & WARREN, B. E. (1954). *J. Appl. Phys.* **25**, 1503.
MÉRING, J. (1949). *Acta Cryst.* **2**, 371.
STOKES, A. R. (1948). *Proc. Phys. Soc.* **61**, 382.
WARREN, B. E. (1955). *Acta Cryst.* **8**, 483.
WARREN, B. E. & AVERBACH, B. L. (1952). *J. Appl. Phys.* **23**, 497.
WILSON, A. J. C. (1942). *Proc. Roy. Soc.* A, **180**, 277.